A self-method for resolving the problem of apparent LWIR emissivity for quantitative thermography at ordinary temperatures

Olivier Riou, Pierre-Olivier Logerais, Fabien Delaleux, Jean-Félix Durastanti

http://dx.doi.org/10.21611/qirt.2014.115

A self-method for resolving the problem of apparent LWIR emissivity for quantitative thermography at ordinary temperatures

by Olivier RIOU, Pierre-Olivier LOGERAIS, Fabien DELALEUX, Jean-Félix DURASTANTI

CERTES, Université Paris Est Créteil, IUT Sénart-Fontainebleau, rue Georges Charpak, F-77567 LIEUSAINT
olivier.riou@u-pec.fr

Abstract

In a previous work, we succeeded in connecting normal LWIR apparent emissivity to the spectral one of an aluminium nitride ceramic plate. We showed a good agreement with the assumption of spectral bandwidth of the used IR system. Our aim in this paper is to justify the considered spectral band [7.5µm, 12µm]. Hence we have developed an analyzer of IR system. The analyzer proceeds by comparing thermosignals with integrated blackbody radiance and adapts spectral bandwidth in order to minimize the dispersion from linearity of the characteristic thermosignals / integrated radiance over a temperature range of the IR system. The capacities of the analyzer are tested for 6 commercial cameras. Each of these systems exhibits a similar formatting process implemented during the thermogram recording. The effective spectral bandwidth exhibits plausible values. It varies significantly from one model to the other and the residual non-linearity is connected to the NETD of the IR system. Applied to the same system which served to characterize the apparent emissivity, the analyzer permits to quantify the effective spectral band. We obtain an excellent agreement between the classical model of apparent emissivity and measurement, both in terms of accuracy and in terms of temperature dependence. The absolute error is 0.005 for emissivity and the temperature coefficient is less than 6 10^{-5} $°C^{-1}$ within the temperature range [40°C, 130°C].

1. Introduction

In quantitative thermography, the apparent emissivity and the reflected temperature have a determining role in the accuracy of the non-contact temperature measurement. According to the typical procedure of temperature measurement, any operator is required to find out and enter only these two values in the microcomputer system. Due to the integration of infrared systems and their current use, operators are constraint to enter an emissivity value in a purely functional goal. Therefore, it is likely that most operators of thermography don't exactly know the relevance of the emissivity they employ. Quantifying the apparent emissivity remains a difficult problem for thermography. Its value depends not only on the emission properties of the target (spectral emissivity, state surface, thickness...), but also on the spectral characteristics of the IR system (bandwidth detection, spectral responsivity of the IR system...) and on the view angle. Because of these sensibilities to functional parameters of the system, apparent emissivity must be considered as an artefact.

A relevant approach to calibrate apparent emissivity is then to determine in situ this parameter using the IR system itself. One can do this by utilizing the classical model of the emitter and the calibration curve in use implicitly in any IR system. The method was tested successfully to characterize the normal LWIR apparent emissivity of an aluminium nitride ceramic plate in the temperature range [40, 550°C] [1]. For this type of materials, apparent emissivity exhibits a tight temperature dependence. By using the classical model of apparent emissivity [2] and by taking into account both the spectral emissivity of aluminium nitride ceramic and the spectral response of the IR sensor, we modelled our apparent emissivity measurement [3]. To apply the model, we need to know with exactness the lower and the higher boundaries of the spectral band of the camera used. Unfortunately, the available information "spectral range" is insufficient to meet this need: most manufacturers of IR systems indicate normalized spectral band without detail. One can understand the lack of information if we assume that only thermosignals interest the manufacturers. They can adapt their products to specific uses whatever the detectivity of the sensors by varying the integration time. Spectral bandwidth appears then strictly indicative and it is used only to differentiate the utilization domain of short waves and long waves IR systems.

To overcome this key problem, we have developed a computer tool to determine the spectral band of infrared systems utilizing only the raw data provided by the operating system itself. The method is based on analysis of the characteristic between thermosignals and blackbody radiance integrated within the effective spectral band of the system. The expected characteristic is linear [4]. By shifting the width of the spectral band, we can highlight a unique pair of wavelengths (λ_1, λ_2) which minimizes the dispersion from linearity. The spectral bandwidth [λ_1, λ_2] defines then the effective spectral band used during the calibration process and during the conversion of thermosignals into OS (Object Signal) units when we record a thermogram. The consistency of the analyzer is tested for 6 commercial cameras. Such approach is self-running: it can be implemented for any IR systems with as unique condition to dispose of thermosignals in OS units.

http://dx.doi.org/10.21611/qirt.2014.115

2. Extraction of thermosignals from software capabilities

Thermosignals quantify the spectral energy absorbed by an IR detector during an exposure time over a spectral band of absorption $\Delta\lambda^*$. Its extent depends on the standard packaging of sensor which defines the short wavelength cut-off at 7.5µm and on the bolometer responsivity threshold which defines the long wavelength cut-off which is conventionally indicated as varying from 13.5µm to 14µm by the manufacturer.

Thermosignals are connected to a standard of radiation during the calibration process. Calibration refers to the set of operations which establish the relationship between the spectral radiation absorbed by each detector and the corresponding known value of spectral blackbody radiation emitted by the source at temperature T over the effective spectral band $\Delta\lambda$. The latter can differ from the absorption one, depending on a number of functional parameters of the IR system such as the temperature range, the conversion range of thermosignals into binary digits and the noise level of the FPA.

To become usable in post-processing treatments, thermosignals are commonly formatted in "object signal" unit (OS). Object Signals refer to the equivalent radiative energy supposed to be emitted by a perfect emitter at a blackbody temperature T_{BB}. Temperatures can then be easily computed from the recorded thermosignals by knowing the effective spectral bandwidth of the system together with the blackbody radiative law. This approach can be generalized to any IR systems if we assume that reverse process is implemented during the record of the thermograms (i.e. conversion of thermosignal in OS). The steps of extraction of thermosignals are done by software: we first record the value of apparent temperatures on a line which display a large temperature distribution. By changing the unit of representation, we record the corresponding Object Signals. The characteristic Object Signals / apparent temperature represent then the calibration curve of the system. Object Signals are insensitive to object parameters which is hence the case for thermosignals which are an overall energy measurement. Concerning the apparent temperature, we must take care to set the "emissivity" to 1. Other parameters like the atmospheric transmittance and any additional optic transmittance should be set to 1 respectively.

3. Identification of the spectral band of the IR system

The method implemented in the analyzer is based on analysis of the characteristic between thermosignals and integrated blackbody radiance within an adjustable spectral bandwidth $\Delta\lambda$. By imposing a linear behaviour, we can highlight a unique pair of wavelengths (λ_1, λ_2) by minimizing the peak dispersion to linearity. The routine is shown in figure 1.

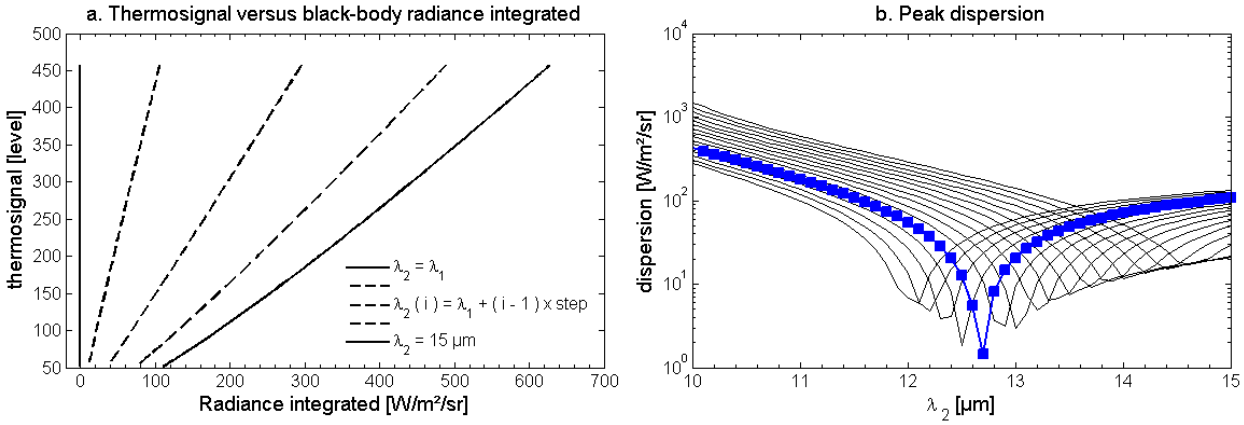

Fig 1. *Routine of analysis of spectral band applied to the Thermacam E300 camera for the temperature range [-20°C, 120°C]*

For each apparent temperature, we first calculate the spectral radiance of the blackbody. Secondly, we calculate the integral of radiance over a bandwidth $\Delta\lambda$. By shifting the width of the spectral band by step of $\delta\lambda$, we linearize the characteristic of the thermosignals versus integrated radiance (figure 1a) and we deduce the peak dispersion between the raw thermosignal and the linearized one (figure 1b). During the process, the lower limit λ_1 ranges from 7 to 9 µm ($\Delta\lambda_1$ = 2 µm) and the upper limit λ_2 varies from λ_1 to 15 µm ($\Delta\lambda$ = 8 µm). As shown in figure 1b, we can highlight a narrow band of wavelengths in which a unique pair of wavelengths (λ_1, λ_2) minimizes the peak dispersion.

The sampling of source data (thermosignals and apparent temperatures) poses a problem. To compare the characteristics, the calculus of integrated radiance should be done for the same sampled values of temperatures like those for thermosignals. To solve this problem, the integration of the spectral radiance is performed over a regular temperature vector [θ_1, θ_2] by step of $\delta\theta$ and we used with this aim an interpolating method to sample the values of integrated radiance according to those of the apparent temperatures. The interpolate method used is the piecewise cubic hermite interpolating polynomial (PCHIP) one. The advantage of this method compared to the others tested (polynomial

http://dx.doi.org/10.21611/qirt.2014.115

of high degrees or spline interpolating methods) is that it is strictly monotonous. The evaluation of radiance integrated uses the trapezoidal integration method over a regular vector [λ_1, λ_2] (figure 1a).

The sensibility of the analyzer to $\delta\theta$ is weak: it shows no change on lower and upper limits of spectral bandwidth and marginally affects only the residual peak dispersion (<0.1%). It is an entirely different matter with $\delta\lambda$: the discretization distorts the determination of the pair of wavelengths (λ_1, λ_2) together with the residual peak dispersion. Figure 2 depicts the sensitivity of these parameters with $\delta\lambda$.

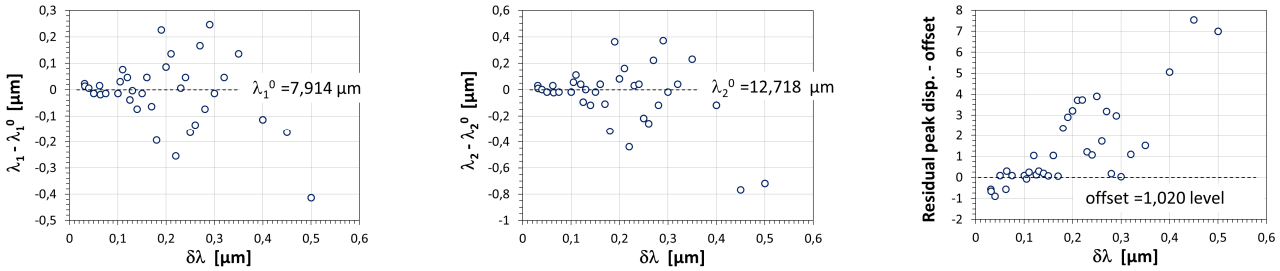

Fig. 2. *Sensitivity of lower and upper limits of spectral bandwidth together with the residual peak dispersion*

We observe a convergence below $\delta\lambda$ = 0.1 µm for both λ_1 and λ_2 whereas the minimum peak value displays more versatility. The value of the maximum peak value can be compared to sensitivity of the thermosignal / apparent temperature which is roughly 2 OS/°C at 30°C and gives a maximum peak temperature dispersion of 0.5°C. To test the robustness of the analyzer, we compare a set of $\delta\lambda$ both integer division of $\Delta\lambda_1$ = 2 µm and $\Delta\lambda$ = 8 µm (ex $\delta\lambda = 1/2^n$, n = 1 to 4): it allows an evaluation under the same conditions of the parameters with a multiple resolution. We note no change in the performances. With the aid of this analyzer, it is then possible to evaluate the pair (λ_1, λ_2) with an uncertainty ± $\delta\lambda$. The uncertainty of the residual peak value is ± 0.5 OS.

4. Test on commercial cameras

The analyzer is now applied for 6 commercial cameras. The main characteristics of each model, derived from datasheets, are presented in table 1. Each camera is tested maintaining $\Delta\lambda_1$ = 2 µm and $\Delta\lambda$ = 8 µm whereas $\delta\lambda$ = 0.1 µm which is a good compromise between exactitude and processing time. Tests are performed over a temperature range which can differ from the nominal one (table 2). Together with the pair of wavelengths (λ_1, λ_2) which minimizes the dispersion, we also report the residual peak equivalent temperature (equal to the ratio of the residual peak dispersion by sensibility at 30°C), the slope of the characteristic thermosignal versus integrated radiance and the value at the origin of these characteristics. From the residual peak value, it is possible to deduce a value of pseudo-NETD (Net Equivalent Temperature Difference) if we assume that standard deviation (NETD) is approximately the ratio of peak value divided by 3. The uncertainty on each value is quantified by comparing the results obtained for the two nearest bands $\lambda_{1/2}$ ± $\delta\lambda$. Uncertainty then corresponds to the standard deviation of the difference of each result compared to those obtained in the band [λ_1, λ_2]. The results of the analyzer are shown in table 2.

The latter shows us that lower and upper limits of spectral bandwidth differ from one model to the other while the NETD is quite similar to those found on datasheets, except for Thermacam E45 for which the temperature range tested is probably too narrow and for Thermacam P65 for which the thermograms had probably been recorded between two NUC (non-uniformity correction). By the single hypothesis of linearity of thermosignal versus integrated blackbody radiance, we highlight that the formatting process is performed so that the thermosignal corresponds directly to the integrated radiance for any IR systems. The case of Thermacam E300 is interesting: this system exhibits two different spectral bands according to its temperature ranges. It is not a surprise to note that the flux emitted from a blackbody at 300°C (middle temperature range) is roughly 6 times higher than the one emitted from a blackbody at 60°C. Assuming that the upper limit of detectivity is 14 µm, 95% of a thermosignal value corresponding to an emitter temperature of 60°C is provided in the band [7.5µm, 13µm]. For an emitter temperature of 300°C, 90% of a thermosignal value is achieved in the band [7.5µm, 12µm]. Above these upper limits, spectral radiance contributes then marginally to the thermosignals and its detection is limited by the corresponding residual peak value displayed in table 2. Concerning the connection of temperatures, we tested the sensitivity of apparent temperature minus the blackbody temperature (which served to calculate the blackbody spectral radiance) with the spectral bandwidth varying from $\lambda_i \pm 2\delta\lambda$. The test is applied to the Thermacam E 300 over the temperature range [50, 550°C]. The result is shown in figure 3. Figure 3 highlights an absolute dispersion of 0.5°C on the temperature range and a significant sensitivity to the spectral bandwidth which justifies the bandwidth found by the analyzer.

One can conclude from this set of independent tests that despite the formatting in OS units, thermosignals are unambiguously connected with blackbody emission and apparent temperature with blackbody temperature. The connection is realized for the only one effective spectral band found by the analyzer. To avoid any misunderstanding, the

http://dx.doi.org/10.21611/qirt.2014.115

analyzer does not identify the spectral band of absorption: it identifies the spectral band used during the formatting of the thermosignals into digital levels.

Table 1. *Models and main characteristics of tested cameras*

Model	Temperature range	Spectral range	Array size (sensor)	NETD @ 30°C
Thermacam E300	[-20°C, 120°C]	[7.5 µm, 13 µm]	320 x 240 (microbolometers)	0.1 °C
	[80°C, 500°C]	[7.5 µm, 13 µm]	320 x 240 (microbolometers)	-
Thermacam E4	[-20°C, 250°C]	[7.5 µm, 13 µm]	160 x 120 (VOx microbolometers)	0.12 °C
Thermacam E45	[-20°C, 250°C]	[7.5 µm, 13 µm]	160 x 120 (VOx microbolometers)	0.1 °C
NEC TH 9100	[-40°C, 500 °C]	[8 µm, 14 µm]	320 x 240 (microbolometers)	0.1 °C
Thermacam P65	[-40°C, 500 °C]	[7.5 µm, 13 µm]	320 x 240 (microbolometers)	0.08 °C

Table 2. *Results of the analyzer*

Model	temperature range tested	λ_1 µm	λ_2 µm	Slope OS / $Wm^{-2}sr^{-1}$	ΔSlope	value at origin OS	ΔValue	Residual peak value @30°C	Pseudo NETD @30°C
Thermacam E300	[-30°C, 130°C]	7,90	12,70	0,997	0,014	0,190	0,604	0,464	0,15
	[50°C, 550°C]	7,70	12,10	0,999	0,011	-7,553	2,561	-	-
Thermacam E4	[-30°C, 220°C]	8,30	13,20	1,001	0,012	-1,130	0,774	0,467	0,16
Thermacam E45	[20°C, 70°C]	7,80	12,60	1,004	0,015	-0,612	0,637	0,161	0,05
NEC TH 9100	[-10°C, 120°C]	6,90	13,70	0,999	0,011	-0,603	0,707	0,372	0,12
Thermacam P65	[-10°C, 550°C]	7,60	11,90	1,000	0,012	-1,524	1,542	0,683	0,23

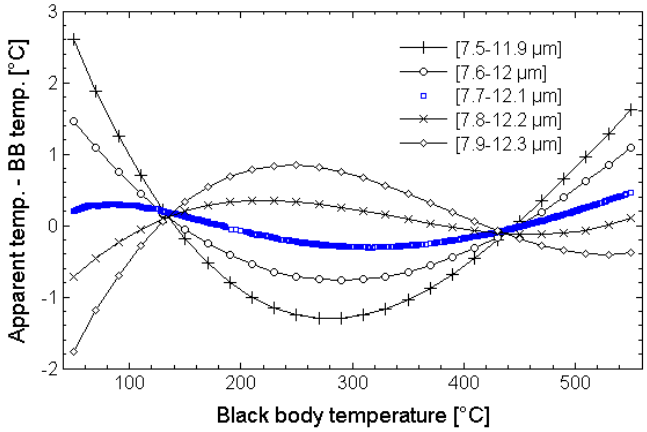

Fig. 3. *Dispersion of apparent temperature compared to blackbody temperature for five spectral bandwidths centred on [7.7, 12.1µm]*

5. Apparent emissivity calculation

From the literature, we can find a general formulation for apparent emissivity [2]:

$$\varepsilon_{\Delta\lambda}(T) = \frac{\int_{\lambda_1}^{\lambda_2} \varepsilon(\lambda, T)\, L^0(\lambda, T)\, R(\lambda)\, d\lambda}{\int_{\lambda_1}^{\lambda_2} L^0(\lambda, T)\, R(\lambda)\, d\lambda} \quad \textbf{(1)}$$

http://dx.doi.org/10.21611/qirt.2014.115

where $\varepsilon_{\Delta\lambda}(\lambda,T)$ is the spectral emissivity of the target, $L^{o}_{\Delta\lambda}(T)$ is the blackbody radiance integrated within the spectral band of the IR system and $R(\lambda)$ is the spectral responsivity of the IR system. This definition leads to an apparent emissivity independent of the wavelength (but dependent on the spectral band of the system) and dependent on the temperature [3]. It should be noted that such dependence is not observed in the case of a grey emitter even though the IR system presents a selective response.

As equation (1) states, apparent spectral emissivity can be defined as the product of the spectral emissivity of the target by the spectral response of the sensors. In microbolometer uncooled focal plane array, the temperature detection is commonly provided by a thermosensitive coating such as vanadium oxide (VOx) or amorphous silicon (a-Si) built with a quarter wave optical. Without specification about the type of sensor used, we are forced to test the two possibilities. Fortunately, the spectral response has been found in the literature (VOx sensor in reference [5] and of a-Si one in reference [6]). For each of them, spectral response is characterized by absorptivity with the aid of an IR spectrometer equipped with an integration sphere or by detectivity (FTIR spectrometer). The first method (reflectivity) takes the fill factor into account.

6. Comparison of apparent emissivity model and measurement

A thermographic approach was used to determine the temperature of an aluminium nitride hot plate as a glass substrate heater for depositing thin films by spray CVD (Chemical Vapour Deposition). The apparent emissivity was measured in situ by using the Thermacam E300 camera within the temperature range of [40°C, 540°C] with a better than 3% accuracy. Absolute value of apparent emissivity was found in agreement with spectrometric values up to 120°C. Dependence on temperature was highlighted. A complete study of this dependence was done [3]. Two major assumptions concerning the exact spectral bandwidth and the detecting technology of the camera were necessary to fit our data to the model of apparent emissivity. The model can then be implemented with the aid of the result presented in the previous sections. The comparison between the model and our measurements is shown in figure 4.

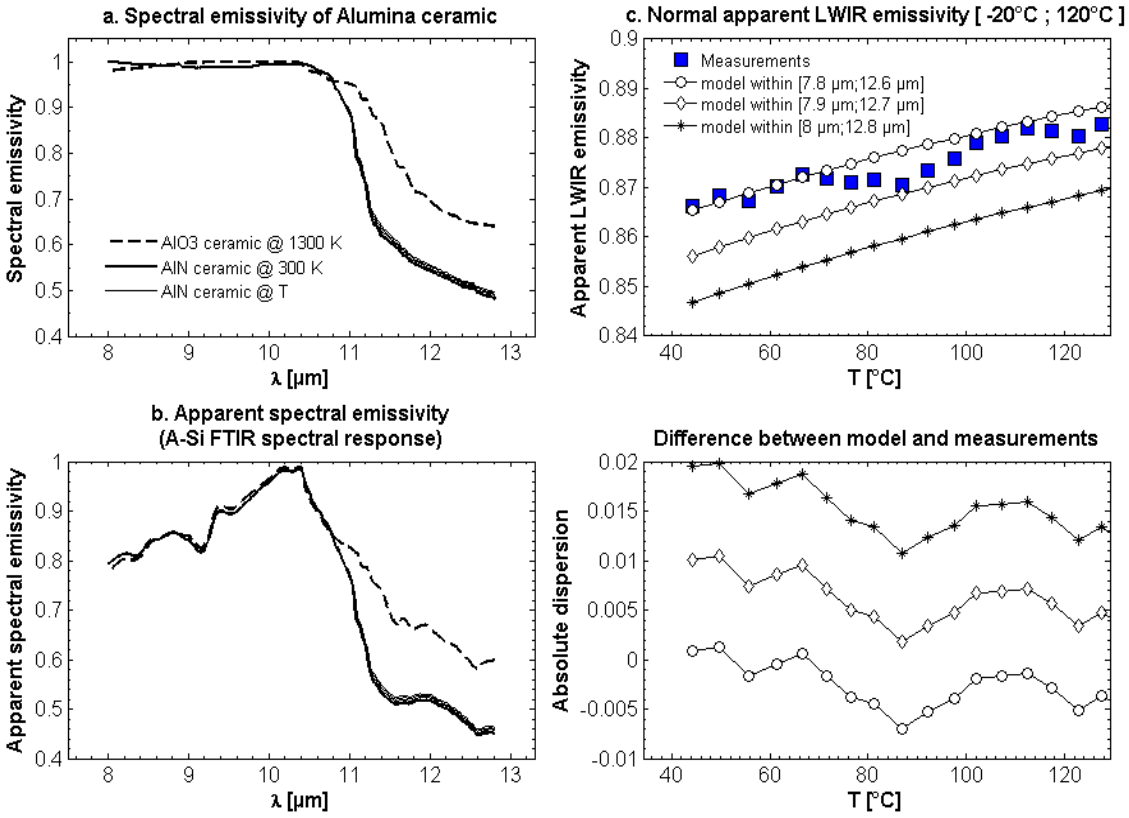

Fig.4. *Model of apparent emissivity applied to measured apparent emissivity of aluminium nitride ceramic*

The sequences of the calculations are the following: emissive properties of aluminium nitride plate were measured by an integral sphere method in the range [2, 25µm]. Measurements are done at 300 K using the CERTES – UPEC spectrometer facilities. To take into account intrinsic variations of the spectral emissivity of AlN plate ceramic as a function of temperature, we quantified the variations observed on a ceramic of aluminium oxide at 1300 K [7]. Assuming that the spectral emissivity varies linearly with temperature, we calculated the rate of variation for each wavelength. We applied this dependence to the spectral emissivity of ceramics at the same temperatures which were used to evaluate

http://dx.doi.org/10.21611/qirt.2014.115

the apparent emissivity. The result is shown in figure 4a. By testing the two detection technologies, we observe that the FTIR response and integral sphere response of a-Si sensor best fits the apparent emissivity measurements (the agreement is close to those obtained from the rectangle window). The apparent spectral emissivity is depicted in figure 4b. We finally compared the measured apparent emissivity to the ones provided by equation (1) over the three spectral bandwidth relative to the camera used for the characterization. The result is displayed in figure 4c. Measurement of apparent emissivity is then subtracted to the one done by the model (figure 4d).

With the assumption of a-Si uncooled microbolometers IRFPA, the difference exhibits an absolute value of less than 0.005 (0.6%) and a temperature coefficient of 6 10^{-5} /°C which is insignificant and it indicates that temperature dependence is perfectly reproduced over the entire temperature range [40, 120°C]. The case of VOx IRFPA displays an absolute dispersion of 0.02 (2.5%) and a temperature coefficient of 10^{-4} /°C. Keeping in mind these limits, the spectral bandwidth done by the analyzer can be implemented successfully to calculate apparent emissivity from the spectral emissivity. It implies also the validity of the radiometric equation for ordinary temperatures which is used implicitly in our measurements of apparent emissivity.

7. Conclusions

In this paper, we implement an analyzer of IR system with the aim of determining its effective spectral bandwidth. The analyzer proceeds by comparing the thermosignals with integrated blackbody radiance and adapts spectral bandwidth in order to minimize the dispersion from linearity of the characteristic thermosignals / integrated radiance over a temperature range of the IR system.

The method is self-running. The analyzer uses only thermosignals provided from software capabilities. After having demonstrated the connection of thermosignals with blackbody radiative law and apparent temperature with blackbody temperature, we tested the capacities of the analyzer for 6 commercial cameras. Each of these systems exhibits a similar formatting process implemented during the thermogram recording. The effective spectral bandwidth exhibits plausible values. It varies significantly from one model to the other and the residual non-linearity is connected to the NETD of the IR system.

We use the analyzer to determine the spectral bandwidth of a commercial 320×240 microbolometer uncooled IRFPA camera which had already served to characterize the normal LWIR apparent emissivity of an aluminium nitride ceramic plate using. Model of apparent emissivity matches best our apparent emissivity measurements. An agreement better than 0.6% in absolute value and a less than 0.006 % /°C dispersion over the entire temperature range [40, 120°C] is highlighted. These results prove the consistency of our apparent emissivity measurements up to 120°C and consequently validate the determination method of apparent emissivity implemented. This method can hence be implemented without restriction for quantitative thermography.

REFERENCES

[1] Olivier Riou, Pierre-Olivier Logerais, Vincent Froger, Jean-Félix Durastanti & Anne Bouteville. Thermal study of an aluminium nitride ceramic heater for spray CVD on glass substrates by quantitative thermography, Journal of Quantitative InfraRed Thermography 10 (2) (2013) 159-171

[2] K. Chrzanowski. Problem of determination of effective emissivity of some materials in MIR range, Infrared Physics & Technology 36(3) (1995) 679–684

[3] Olivier Riou, Pierre-Olivier Logerais, Jean-Félix Durastanti. Quantitative study of the temperature dependence of normal LWIR apparent emissivity, Journal of Infrared Physics & Technology 60 (2013) 244–250

[4] Olivier Riou, Stéphane Berrebi, Pierre Brémond. Non uniformity correction and thermal drift compensation of infrared camera, Thermosense XXVI, Proc. SPIE 5405 (2004) 294-302

[5] N. Liberatore, A. Pifferi, S. Perri, M. E. Marini. Test bench for IRFPA based on CMT and microbolometer, Infrared Physics & Technology 43(3–5) (2002) 291–296.

[6] J. L. Tissot, C. Trouilleau, B. Fieque, A. Crastes, O. Legras. Uncooled microbolometer detector: recent developments at ULIS, Opto-Electronics Review 14(1) (2006) 25-32.

[7] O. Rozenbaum, D. De Sousa Meneses, P. Echegut. Texture and Porosity Effects on the Thermal Radiative Behavior of Alumina Ceramics, Int J Thermophys 30 (2009) 580-590.